Modeling of Fouling on Packings in Absorption Columns

Arthur Heberle and Karlheinz Schaber
Institut für Technische Thermodynamik und Kältetechnik, Universität Karlsruhe, 76128 Karlsruhe, Germany

A model describing the fouling in irrigated columns with random packings was applied successfully to the description of the increase in pressure drop when fouling occurs during the absorption of CO_2 in a suspension of $Ca(OH)_2$. It is based on the Darcy–Weisbach law and the channel model. A mass balance around a fouling layer on the packings leads to a time-dependent equation including the hydraulic radius from the channel model. A removal term is introduced in the fouling model. To approach the experimental results, the removal term had to be extended by an empirical parameter. It can be interpreted as a removal efficiency factor and is obtained by easy numerical fitting.

Introduction

In many industrial absorption processes it often would be desirable to use suspensions as scrubber solutions. When deposits are likely, jet scrubbers or spray towers, for instance, are used instead of packed columns. But the energy demand per NTU (Number of Transfer Units) of an absorbed component in a jet scrubber or spray tower is higher than the specific energy demand in an absorption column. According to Schaber (1987), jet scrubber absorption of sulphur dioxide in a NaOH solution demands about 0.18 up to 0.5 Wh/m^3 per NTU. In comparison, the specific energy demand of the same absorption in a packed column is 0.11 up to 0.15 Wh/m^3 per NTU.

Fouling can be defined as the unwanted formation and accumulation of deposits on surfaces. There is always a competition between adhesion forces and removal forces. Fouling causes serious problems. Generally, fouling cannot be predicted or calculated in advance. If fouling occurs, oversized plants must be established to compensate for the impact of the fouling (higher capital costs); this makes the energy demand higher because the pressure drop becomes higher. Often expensive maintenance (cleaning) is necessary, and interruption of plant operation leads to losses of production. Fouling costs money.

If one reviews up-to-date studies, one will find a lot of investigations on fouling in heat exchangers (e.g., Bott, 1995; Crittenden et al., 1992; Epstein, 1983; Taborek et al., 1972a,b), but there are very few investigations on fouling in absorption columns with packings, as already mentioned in Heberle et al. (2001). In most articles, the negative impacts of fouling in columns are described or advice is given on how to reduce fouling (e.g., Bravo, 1993; Martin, 1988). In Chen et al. (1995) investigations were made on fouling on sieve trays. There, a first semiempirical model for sieve trays has been presented to outline the pressure drop as a function of time.

First, Heberle et al. (2001) performed closer investigations on fouling in an absorption column with packings. The pressure drop Δp measured in the packing column was chosen as an indicator for fouling effects. Among several other different ways to reflect fouling, such as measuring the weight of the packing or the thickness of the deposit on the packing surface, pressure drop seems to be the easiest method.

Three fouling mechanisms can be identified in the absorption process: crystallization fouling, precipitation fouling, and particulate fouling. Crystallization fouling can be defined as the formation of deposits by the removal of a solvent (evaporation). The difference between precipitation and crystallization is often not very clear. According to Söhnel and Garside (1992), precipitation is the rapid crystallization of slightly soluble substances, and it generally involves the simultaneous and rapid occurrence of nucleation and growth, as well as the presence of secondary processes, such as aging and agglomeration. Chemical-reaction fouling, corrosion fouling, and biological fouling, which can occur as well, are not part of these investigations. It should be mentioned that

Correspondence concerning this article should be addressed to K. Schaber.

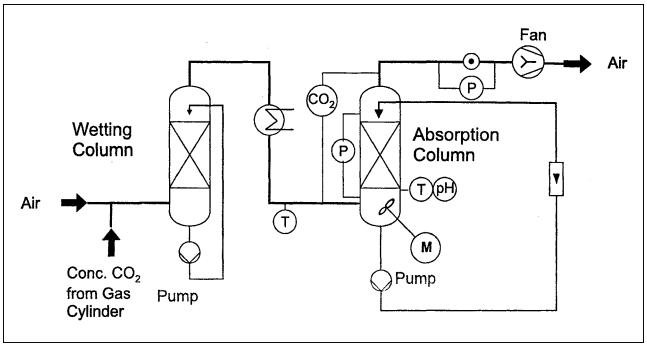

Figure 1. Experimental set used for fouling experiments (Heberle et al., 2001).

sedimentation might occur in superposition with the two other mentioned mechanisms, but it is not a significant factor. The most dominant mechanism is precipitation fouling.

The research work presented deals with the modeling of the pressure drop caused by fouling in an absorption packed column. It was possible to describe the fouling mechanism based upon the Darcy–Weisbach law and upon the channel model. The resulting equation contains three parameters that are fitted to experimental data by a simple algorithm.

Experimental Set

In order to carry out the experiments, a plant was used that consisted of an absorption column and a humidifying column (Heberle et al., 2001). The absorption column has a diameter of 0.15 m and a packing height of about 1.06 m. The scrubber solution is circulated. An IR photometer can be used to measure the temperatures of the inlet and outlet gas, of the scrubber solution, and the pH-value, as well as the inlet and outlet carbon dioxide concentration.

Loss of water by evaporation can be compensated for by external water feeding. The pressure drop, Δp, is measured by a differential pressure manometer. The humidifying column can be used for the saturation of the inlet air. When particulate fouling and/or crystallization fouling were checked, the humidifying column was switched on. The experiments were performed at environmental conditions, with an average gas inlet temperature of about 20°C.

A selection of the experimental results is presented here. The liquid load u^L has been adjusted in the range from 11.32 to 39.61 $m^3/(m^2 \cdot h)$, the gas velocity w^G from 0.5 to 1.3 m/s, and the CO_2-inlet concentration from about 500 to 2,000 ppm. Packings of the Hiflow 15-7 PP type (Rauschert Company, Germany) were used for fouling investigations. To simulate precipitation fouling, a 3.5 Mass-% $Ca(OH)_2$ suspension has been used. The reaction of CO_2 and $Ca(OH)_2$ yields $CaCO_3$.

All experiments were performed as a semibatch operation, that is, a continuous gas stream (air and carbon dioxide) was introduced to a circulated scrubber solution of a constant volume (0.025 m^3). All experiments took 10 h.

Theory

For a better comparison of the increase in the pressure drops, it is recommended that a fouling factor, R_F, be defined. This factor is a quotient of pressure drop $\Delta p(t)$ at time $t \geq 0$, and pressure drop Δp_0 at time $t = 0$, when no fouling has occurred in a clean packing:

$$R_F = \frac{\Delta p(t)}{\Delta p_0}. \tag{1}$$

According to other publications (for example, Bott, 1995; Crittenden et al., 1992; Epstein, 1983), the net fouling rate used to describe fouling in heat exchangers,

$$\frac{dR_F}{dt} = \dot{\Pi}_d - \dot{\Pi}_r, \tag{2}$$

can be used to describe fouling in absorption columns as well. Equation 2 contains a deposition term $\dot{\Pi}_d$ and a removal term $\dot{\Pi}_r$.

In order to calculate a pressure drop, Δp, per height, H, it is common to apply the fundamental Darcy–Weisbach law

$$\frac{\Delta p}{H} = \lambda \cdot \frac{\left(w_{\text{eff}}^G\right)^2 \cdot \rho^G}{2 \cdot d_h} = \lambda \cdot \frac{\left(F_{\text{eff}}^G\right)^2}{2 \cdot d_h}. \tag{3}$$

This law is based upon the one-phase flow through a channel. Here, d_h represents the hydraulic diameter, ρ^G is the gas density, and λ is the drag coefficient. The effective gas velocity, w_{eff}^G, and an effective F-factor, F_{eff}^G, respectively, include the porosity ϵ, and can be expressed as

$$w_{\text{eff}}^G = \frac{w^G}{\epsilon} \quad \text{and} \quad F_{\text{eff}}^G = \frac{F^G}{\epsilon}. \tag{4}$$

With the introduction of a wall factor K (Brauer and Mewes, 1972) and the dry geometrical specific surface, a_{geo}, the hydraulic diameter, d_h, and the hydraulic radius, r_h, respectively, can be obtained as

$$d_h = 2 \cdot r_h = 4 \cdot \frac{\epsilon \cdot K}{a_{\text{geo}}} = \frac{2}{3} \cdot \frac{\epsilon}{1-\epsilon} \cdot d_P \cdot K. \tag{5}$$

Together with Eqs. 4 and 5, Eq. 3 can be transformed into a general pressure-drop equation for a one-phase flow

$$\frac{\Delta p}{H} = \frac{3 \cdot \lambda}{4} \cdot \frac{1-\epsilon}{\epsilon^3} \cdot \frac{\left(F^G\right)^2}{d_P \cdot K} = \frac{\psi}{3} \cdot \frac{\left(F^G\right)^2}{r_h \cdot \epsilon^2}. \tag{6}$$

In Eqs. 5 and 6 d_P is a particle diameter that has the same value as the diameter of a channel. The drag coefficient, ψ, for a one-phase flow in Eq. 6 is an abbreviation for $3\lambda/4$, and is a function of the Reynolds number Re^G of a gas flow.

A lot of correlations have been suggested for laminar and turbulent flow (e.g., Brauer and Mewes, 1972; Billet and Schultes, 1999; Mackowiak, 1991b). Here we have used only the correlations according to Mackowiak (1991b). Taking the pressure drop equation of Mackowiak (1991a,b) for *irrigated*

packings with a gas flow, that is, two-phase flow,

$$\frac{\Delta p(r_h)}{H} = \left(\psi^{GL}\right)^* \cdot \frac{1-\epsilon_0}{\epsilon_0^3} \cdot \frac{\left(F^G\right)^2}{d_P \cdot K} = \frac{\left(\psi^{GL}\right)^*}{3} \cdot \frac{\left(F^G\right)^2}{r_h \cdot \epsilon_0^2} \tag{7a}$$

with

$$\left(\psi^{GL}\right)^* = \psi^{GL} \cdot \left[1 + \frac{h^L}{1-\epsilon_0}\right] \cdot \left[1 - \frac{h^L}{\epsilon_0}\right]^{-3}, \tag{7b}$$

which is based on Eq. 6 and contains the liquid holdup, h^L. The liquid holdup, h^L, is defined as the ratio of the total liquid volume in a packing, V^L, and the total volume of the packing, V_{tot}. Equation 7a takes into account that the thickness of a liquid film, δ, changes the hydraulic radius, $r_{h,0}$, and thereby the porosity, ϵ_0, of a clean and dry packing. Here, ψ^{GL} is a gas-side drag coefficient for a two-phase flow. Mackowiak (1991a,b) also called ψ^{GL} a "pseudo drag coefficient." In addition, ψ^{GL} is a function of liquid-side Reynolds number Re^L and of the packing type. Mackowiak (1991b) gives several correlation equations for ψ^{GL}.

If *fouling* occurs, the parameters ϵ, r_h, and h^L change and become time-dependent, thus $\Delta p/H$ increases with time t.

When fouling occurs on packings, the dry geometric specific surface, a_{tr}, the void fraction ϵ, and thus the hydraulic radius r_h (see Figure 2) are reduced by the increasing fouling deposit. It is expressed by the thickness x_F. The total volume of the packings does not change at $t \geq 0$. However, the volume of the fouling deposit increases with time. Now a uniform distribution of deposits over the column height, H, is assumed, that is, the hydraulic radius $r_h \neq r_h(H)$. That assumption is needed because there is no information about the deposit distribution throughout the packings.

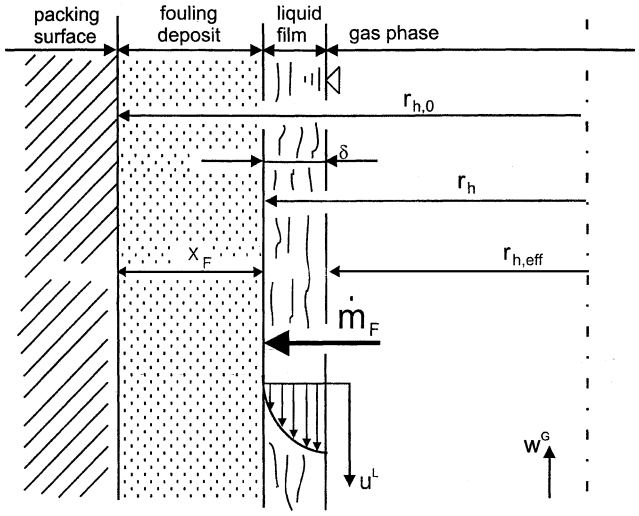

Figure 2. Geometry of a surface when fouling occurs at $t > 0$.

Based on the definition of the void fraction, ϵ, in the channel model for packings the following new equations (Eqs. 8 and 9) for calculating $\epsilon(t)$ and $a_{\text{geo}}(t)$ in a nonirrigated packing with one-phase flow and fouling can be derived:

$$V_{\text{Ch}} = N_{\text{Ch}} \cdot \pi \cdot r_h^2 \cdot H = N_{\text{Ch}} \cdot \pi \cdot r_{h,0}^2 \cdot H \cdot \left(\frac{r_h}{r_{h,0}}\right)^2$$

$$= V_{\text{Ch},0} \cdot \left(\frac{r_h}{r_{h,0}}\right)^2 \Rightarrow \epsilon = \epsilon_0 \cdot \left(\frac{r_h}{r_{h,0}}\right)^2 = \epsilon(t) \tag{8}$$

$$A_{\text{geo}} = N_{\text{Ch}} \cdot 2 \cdot \pi \cdot r_h \cdot H = N_{\text{Ch}} \cdot 2 \cdot \pi \cdot r_{h,0} \cdot H \cdot \left(\frac{r_h}{r_{h,0}}\right)$$

$$= A_{\text{geo},0} \cdot \left(\frac{r_h}{r_{h,0}}\right) \Rightarrow a_{\text{geo}} = a_{\text{geo},0} \cdot \left(\frac{r_h}{r_{h,0}}\right) = a_{\text{geo}}(t). \tag{9}$$

In Eq. 8 V_{Ch} is the volume of a channel, and N_{Ch} is the total channel number. In Eq. 9 a_{geo} represents the dry geometric surface. The porosity ϵ_0 and the dry geometric specific surface $a_{\text{geo},0}$ are values at the time $t = 0$, and can be taken from suppliers' data. Then calculation of the hydraulic radius, $r_{h,0}$, at time $t = 0$, Eq. 5, is possible.

If an irrigated packing with deposits is considered, Eqs. 8 and 9 change into

$$\epsilon_{\text{eff}} = \frac{V_{\text{tot}} - V_{\text{packing}} - V_F(t) - V^L(t)}{V_{\text{tot}}}$$

$$= \underbrace{\frac{V_{\text{tot}} - V_{\text{packing}} - V_F(t)}{V_{\text{tot}}}}_{=\epsilon(t)} - \underbrace{\frac{V^L(t)}{V_{\text{tot}}}}_{=h^L(t)}$$

$$\Rightarrow \epsilon_{\text{eff}}(t) = \epsilon_0 \cdot \left(\frac{r_h}{r_{h,0}}\right)^2 - h^L(t) \tag{10}$$

$$a_{\text{eff}}(t) = a_{geo} \cdot f\left(h^L, \epsilon_{\text{eff}}\right) \tag{11a}$$

$$= a_{\text{geo},0} \cdot \left(\frac{r_h}{r_{h,0}}\right) \cdot f\left(h^L, \epsilon_{\text{eff}}\right), \qquad h^L = h^L(t) \tag{11b}$$

Equation 10 contains the total volume of the packing, V_{tot}, the packing without any voidage, V_{packing}, and the time-dependent volume of the fouling deposit, $V_F(t)$, and of the liquid holdup, $V^L(t)$, which have to be subtracted there. According to Mackowiak (1991a,b), the liquid holdup is $h^L(t) \sim (B^L)^m$ with a fitting parameter, m. The nondimensional liquid load B^L is also a function of the porosity $\epsilon_{\text{eff}}(t)$.

Equation 11a contains a correction factor, $f(h^L, \epsilon_{\text{eff}})$, referred to in Mackowiak (1991b), and considers the decrease in the hydraulic radius, r_h, by a liquid film of the thickness δ, see Figure 2. Extending Eq. 11a with Eq. 9 yields Eq. 11b. Moreover, in Mackowiak (1991a,b) a relation can be found between ψ^{GL} and $(\psi^{GL})^*$ (see Eq. 11c), with the already mentioned correction function $f(h^L, \epsilon_{\text{eff}})$:

$$\psi^{GL} = \left(\psi^{GL}\right)^* \cdot \frac{f\left(h^L, \epsilon_{\text{eff}}\right)}{1 + h^L/(1-\epsilon_{\text{eff}})}. \tag{11c}$$

If Eqs. 5, 10, 11b, and 11c are put into a modified equation

based on Eq. 7a,

$$\frac{\Delta p(r_h)}{H} = \left(\psi^{GL}\right)^* \cdot \frac{1-\epsilon_{\text{eff}}}{\epsilon_{\text{eff}}^3} \cdot \frac{\left(F^G\right)^2}{d_{P,\text{eff}} \cdot K} = \frac{\left(\psi^{GL}\right)^*}{3} \cdot \frac{\left(F^G\right)^2}{r_{h,\text{eff}} \cdot \epsilon_{\text{eff}}^2}, \quad (12a)$$

the pressure drop in irrigated packings with fouling becomes

$$\frac{\Delta p(r_h)}{H} = \frac{\psi^{GL}(t)}{3} \cdot \frac{\left(F^G\right)^2}{\epsilon_0^2 \cdot r_{h,0}^2} \cdot \frac{K_0}{K(t)} \cdot r_h(t) \cdot \left[1 + \frac{h^L(t)}{1-\epsilon_0}\right] \cdot \left[\left(\frac{r_h(t)}{r_{h,0}}\right)^2 - \frac{h^L(t)}{\epsilon_0}\right]^{-3}. \quad (12b)$$

In Eq. 12a both the effective particle diameter, $d_{P,\text{eff}}$, and the hydraulic radius, $r_{h,\text{eff}}$, consider the hydraulic radius, r_h, including the deposit thickness, x_F, and the liquid film thickness, δ, caused by irrigation, that is, $r_{h,\text{eff}} = r_h - \delta$ (see Figure 2).

The correction function, $f(h^L, \epsilon_{\text{eff}})$, disappears after Eq. 12a is rearranged. The wall factors K_0 and $K(t)$ are mentioned in Eq. 12b. The expression can be simplified by assuming $K(r_{h,\text{eff}}) \approx K(r_h)$ (i.e., $\delta \ll r_h$) and $K(r_h) \approx K(r_0)$ (i.e., $K \neq K(t)$). Thus $K_0/K(t) \approx 1$.

When the fluid dynamic characteristic nondimensional numbers, such as Re^G, Re^L, Fr^L, We^L/Fr^L, and B^L, are known, the liquid holdup, $h^L(t)$, and the two-phase drag coefficient, ψ^{GL}, can be calculated by using the correlations of Mackowiak (1991b). As $\epsilon = \epsilon(t)$, $a_{\text{geo}} = a_{\text{geo}}(t)$, and $d_p = d_p(t)$, the nondimensional numbers are time-dependent, as well.

The hydraulic radius, $r_h(t)$, in Eq. 13 can be calculated with the aid of a mass balance around the fouling deposit

$$\frac{dr_h(t)}{dt} = -\frac{\dot{m}_F(t)}{\rho_P \cdot A_{\text{geo}}(t)} \quad (13)$$

with

$$\dot{m}_F = \dot{m}_d - \dot{m}_r. \quad (14)$$

If the decisive fouling mechanism is known, expressions can be found to define the net fouling mass rate, $\dot{m}_F$. In Eq. 14 the net fouling rate, $\dot{m}_F$ is obtained by subtracting the removal mass rate, $\dot{m}_r$, from the deposition mass rate, $\dot{m}_d$. The removal of the deposit is caused by abrasion, erosion, and dissolution.

According to Heberle et al. (2001), fouling caused by precipitation is the most prevalent mechanism in the investigations cited.

In case of *precipitation fouling* (subscript PF), a chemical reaction of the general type (R1) can occur

$$z_A A(g) + z_B B(s) \rightarrow z_P P(s), \quad \text{(R1)}$$

where z_A, z_B, and z_P are stoichiometric coefficients of the components A, B, and P. In the investigation cited, A stands for CO_2, B for $Ca(OH)_2$, and P for $CaCO_3$.

Equation 13 becomes the ordinary first-order differential equation

$$r_h \cdot dr_h = -\frac{\dot{m}_F}{2 \cdot \pi \cdot H \cdot N_{Ch} \cdot \rho_P} dt, \quad (15)$$

with

$$\dot{m}_F = \dot{m}_{F,\,PF} = M_P \cdot \frac{z_P}{z_A} \cdot \dot{N}_A^{\text{abs}}. \quad (16)$$

In Eq. 16 M_P is the molar mass of the product P, and $\dot{N}_A^{\text{abs}}$ is the absorption rate of gas A. The net fouling mass rate, $\dot{m}_F = \dot{m}_{F,PF}$, refers to precipitation fouling. Integration of Eq. 15 with the initial condition, $r_h(t=0) = r_{h,0}$, leads to

$$r_h(t) = \sqrt{r_{h,0}^2 - \frac{M_P \cdot \frac{z_P}{z_A} \cdot \dot{N}_A^{\text{abs}}}{\pi \cdot H \cdot N_{\text{Ch}} \cdot \rho_P} \cdot t}, \quad (17)$$

and, respectively, to the nondimensional form

$$\frac{r_h}{r_{h,0}} = \frac{r_h(t)}{r_{h,0}} = \sqrt{1 - \frac{t}{t^* \cdot N_{\text{Ch}}}} = \sqrt{1 - \frac{t}{t^*}} \quad (18)$$

with $N_{\text{Ch}} = 1$ and

$$t^* = \frac{\pi \cdot H \cdot \rho_P \cdot r_{h,0}^2}{M_P \cdot \frac{z_P}{z_A} \cdot \dot{N}_A^{\text{abs}}}. \quad (19)$$

It is important to assume that $N_{\text{Ch}} = 1$ for all calculations. If a calculated channel number, N_{Ch}, of a certain packing was used at a given column diameter and a given t^*, it would lead to a higher channel number and to a higher ratio, $r_h/r_{h,0}$, at packings of smaller sizes, that is, from the calculation point of view, less fouling would occur on small-size packings than on large-size packings. However, the experiment shows the opposite result.

The parameter t^* can be seen as a characteristic time parameter. At $t = t^*$, the pressure drop becomes infinite. Thus, t^* is a maximum value. Moreover, the higher the absorption rate is, the faster the fouling formation occurs and the lower the value of t^* is.

In reality, a part of the formed product, P, given by the product mass rate, $\dot{m}_P$, will be removed and does not contribute to the deposit on the packings. Thus, a correction is needed that yields an empirical fitting parameter, γ, defined in Eq. 20 as the removal efficiency

$$\gamma = \frac{\dot{m}_P - \dot{m}_{F,PF}}{\dot{m}_P}. \quad (20)$$

The removal efficiency, γ, represents a new and a very important approach. Equation 16 can be extended with the removal efficiency, γ, to

$$\dot{m}_{F,PF} = M_P \cdot \frac{z_P}{z_A} \cdot \dot{N}_A^{\text{abs}} \cdot (1-\gamma). \tag{21}$$

The general relation of $r_h(t)/r_{h,0}$ in Eq. 18 is still valid, but Eq. 19 has changed into

$$t^* = \frac{\pi \cdot H \cdot \rho_P \cdot r_{h,0}^2}{M_P \cdot \frac{z_P}{z_A} \cdot \dot{N}_A^{\text{abs}} \cdot (1-\gamma)}. \tag{22}$$

γ must be fitted to the experimental results. A general correlation for all experimental results should be found. Based upon considerations made by Crittenden and Kolaczkowski (1979) and Taborek et al. (1972a,b), the removal efficiency is influenced by the wall stress, τ_w, a structure parameter, ψ_{Str}^*, and, in addition, by the absorption rate, which has been found to be a major cause of fouling. We now suggest a possible correlation to combine the main influences. In Eq. 23, a mean shear stress, $\bar{\tau}_W$, is used, because the change in shear stress within one single experiment performed under constant operation conditions is not significant (less than 1%), therefore $\tau_W(t) \approx \bar{\tau}_W$

$$\gamma = \left(\frac{\bar{\tau}_W}{\psi_{\text{Str}}^*} \right)^a \left(1 - \frac{\dot{N}_A^{\text{abs}}}{\dot{N}_{A,\max}^{\text{abs}}} \right)^b. \tag{23}$$

Equation 23 is constructed in two parts. The first part reflects the influence of the forces that act on and in the solid deposit. The second part reflects the increasing deposit with increasing mass transfer.

In Eq. 23, $\dot{N}_{A,\max}^{\text{abs}}$ is the maximum absorption rate at the experimental operation conditions presented. It is used to transform the second part into a nondimensional term. At an absorption efficiency $\epsilon_{\text{abs}} = 1$, gas velocity $w^G = 1.0$ m/s, and $y(CO_2)_{\text{in}} \approx 2{,}000$ ppm, a maximum absorption rate of 0.00145 mol/s is calculated. The structure parameter ψ_{Str}^* describes the resistance of the fouling deposit against removal (shearing strength and adhesiveness). According to Hirsch (1997), however, ψ_{Str}^* should be seen as a hypothetical parameter, because exact physical correlations are still unknown: a, b, and ψ_{Str}^* are adjustable parameters.

By using the new Eq. 23 suggested, and depending on the operation conditions, the general relation between the observed experimental results is described as: γ is decreased with decreasing wall stress, increasing absorption rates, and increasing shearing strength and adhesiveness. If the value of the structure parameter is much larger than the value of the wall stress, there will be no significant removal. Then, the deposit has its highest adhesiveness and shearing strength.

Up to now, only precipitation fouling has been considered. In the case of *crystallization fouling* (subscript *CF*), the solubility, S_j, of a solid j and the evaporation rate $\dot{m}_{ev}$ must be taken for the mass balance; see Eqs. 13 and 14. The net fouling rate for crystallization fouling, $\dot{m}_F = \dot{m}_{F,CF}$, becomes

$$\dot{m}_F = \dot{m}_{F,CF} = \sum_j \frac{dm_{F,CF,j}}{dt} = \sum_j \dot{m}_{ev} \cdot S_j \tag{24a}$$

$$\dot{m}_{F,CF} = K_P \cdot \frac{dm_P}{dt} + K_B \cdot \frac{dm_B}{dt} = (K_P \cdot S_P + K_B \cdot S_B) \cdot \dot{m}_{ev}. \tag{24b}$$

The evaporation rate $\dot{m}_{ev}$ is assumed to be constant. In Eq. 24b, K_P and K_B are fitting parameters and can be interpreted as adhesion efficiencies, S_P and S_B are the solubilities of components P and B from reaction (R1). It is assumed that if the evaporation rate, $\dot{m}_{ev}$, is kept constant, Eq. 18 can be applied again, but the characteristic time parameter, t^*, changes into

$$t^* = \frac{\pi \cdot H \cdot \rho_F \cdot r_{h,0}^2}{(K_P \cdot S_P + K_B \cdot S_B) \cdot \dot{m}_{ev}}. \tag{25}$$

The density of the fouling deposit, ρ_F, is a mixture of the density of the components P and B. Chen et al. (1995) did not include a removal term in their investigation. Consequently, there is no removal efficiency in Eq. 24b.

The superposition of precipitation fouling and crystallization fouling provides

$$\dot{m}_F = \dot{m}_{F,PF} + \dot{m}_{F,CF} = M_P \cdot \frac{z_P}{z_A} \cdot \dot{N}_A^{\text{abs}} \cdot (1-\gamma) + (K_P \cdot S_P + K_B \cdot S_B) \cdot \dot{m}_{ev}. \tag{26}$$

Table 1. Characteristic Time Constants: Overview

Case (I): precipitation fouling without removal $\gamma = 0$, with removal $0 < \gamma < 1$	$t^* = \dfrac{\pi \cdot H \cdot \rho_P \cdot r_{h,0}^2}{M_P \cdot \frac{z_P}{z_A} \cdot \dot{N}_A^{\text{abs}} \cdot (1-\gamma)}$
Case (II): crystallization fouling without removal	$t^* = \dfrac{\pi \cdot H \cdot \rho_F \cdot r_{h,0}^2}{(K_P \cdot S_P + K_B \cdot S_B) \cdot \dot{m}_{\text{ev}}}$
Case (III): superposition of (I) and (II)	$t^* = \dfrac{\pi \cdot H \cdot \rho_F \cdot r_{h,0}^2}{M_P \cdot \frac{z_P}{z_A} \cdot \dot{N}_{A,\text{abs}} \cdot (1-\gamma) + (K_P \cdot S_P + K_B \cdot S_B) \cdot \dot{m}_{\text{ev}}}$

Equation 27 yields a modified characteristic time parameter

$$t^* = \frac{\pi \cdot H \cdot \rho_F \cdot r_{h,0}^2}{M_P \cdot \frac{z_P}{z_A} \cdot \dot{N}_A^{\text{abs}} \cdot (1-\gamma) + (K_P \cdot S_P + K_B \cdot S_B) \cdot \dot{m}_{ev}}. \quad (27)$$

All in all, a set of different characteristic time constants, t^*, can be determined, as illustrated in Table 1.

An expression for the fouling factor R_F can be derived from the basic equation (Eq. 12)

$$R_F = \underbrace{\left(\frac{\psi^{GL}}{\psi_0^{GL}}\right)}_{\approx 1} \cdot \left(\frac{r_h}{r_{h,0}}\right) \cdot \underbrace{\left(\frac{K}{K_0}\right)}_{\approx 1} \cdot \frac{(1-\epsilon_0)+h^L}{(1-\epsilon_0)+h_0^L} \cdot \left[\frac{\epsilon_0 - h_0^L}{\epsilon_0 \left(\frac{r_h}{r_{h,0}}\right)^2 - h^L}\right]^3. \quad (28)$$

Liquid flows at $Re^L \geq 12.3$ have been examined. So, in the view of Mackowiak (1991a,b), the two-phase pseudodrag coefficient ψ^{GL} is not a function of the Reynolds number, Re^L, and is therefore time-independent. Re^L is not a function of the packing type. Moreover, we still assume that $K \approx K_0$. Consequently, rearranging Eq. 28 together with Eq. 10 yields the simple fouling equation

$$R_F = \underbrace{\left[\frac{r_h(t)}{r_{h,0}}\right]}_{=A} \cdot \underbrace{\frac{(1-\epsilon_0)+h^L(t)}{(1-\epsilon_0)+h_0^L}}_{=B} \cdot \underbrace{\left[\frac{\epsilon_{\text{eff},0}}{\epsilon_{\text{eff}}(t)}\right]^3}_{=C} \quad (29)$$

Equation 29 consists of three terms, A, B, and C. If the fouling deposit increases, term A decreases. Term B increases when the flow resistance and liquid holdup increased. The third term, C, also increases with time, and the porosity, ϵ, decreases due to the increasing fouling deposit. Term C is limited to the characteristic time parameter, t^*, and C has a pole at $\epsilon_{\text{eff}} \to 0$. The liquid holdup increases with time, while the values for the hydraulic radius decrease. If $t \to t^*$, then $\epsilon_{\text{eff}}(t) \to 0$. A new liquid holdup, h_∞^L, can be defined from Eq. 10. It becomes

$$0 = \epsilon_0 \cdot \left(\frac{r_h}{r_{h,0}}\right)^2 - h_\infty^L \Rightarrow h_\infty^L = \epsilon_0 \cdot \left(\frac{r_h}{r_{h,0}}\right)^2. \quad (30)$$

Calculation of the mean shear stress, $\bar{\tau}_W$, in Eq. 23, which is caused by the downstreaming liquid without taking the gas stream into account, is reflected in the Newton approach

$$\tau_W = -\eta^L \cdot \left(\frac{dw_{\text{film}}^L}{dy}\right), \quad (31)$$

where η^L is the dynamic viscosity and w_{film}^L is the liquid film velocity. For the calculation of the film velocity, an average value, $\bar{w}_{\text{film}}^L$, is taken by considering the Nusselt water skin theory while neglecting the gas stream:

Table 2. Calculated Mean Shear Stress at Different Gas Velocities and Liquid Loads, Constant $y(CO_2)_{\text{in}} \approx 2{,}000$ ppm

	Mean Shear Stress $\bar{\tau}_W$/Pa		
w^G (m/s)	16.98 m³/(m²·h)	28.29 m³/(m²·h)	39.61 m³/(m²·h)
0.5	4.3519	4.7750	5.0737
1.0	4.4025	4.8794	5.2297
1.3	4.4545	(no exp.)	(no exp.)

$$\bar{w}_{\text{film}}^L = \frac{2}{3} \cdot w_{\text{film,max}}^L = \frac{g \cdot \delta^2}{3 \cdot \nu^L}. \quad (32)$$

According to Bornhütter and Mersmann (1993), the thickness of the liquid film δ can be predicted by the cylinder model.

Table 2 provides an overview of the calculated mean shear stress at different operation conditions.

Numerical Algorithm

As already mentioned, only precipitation fouling has been considered in the investigations presented. Thus, for model-

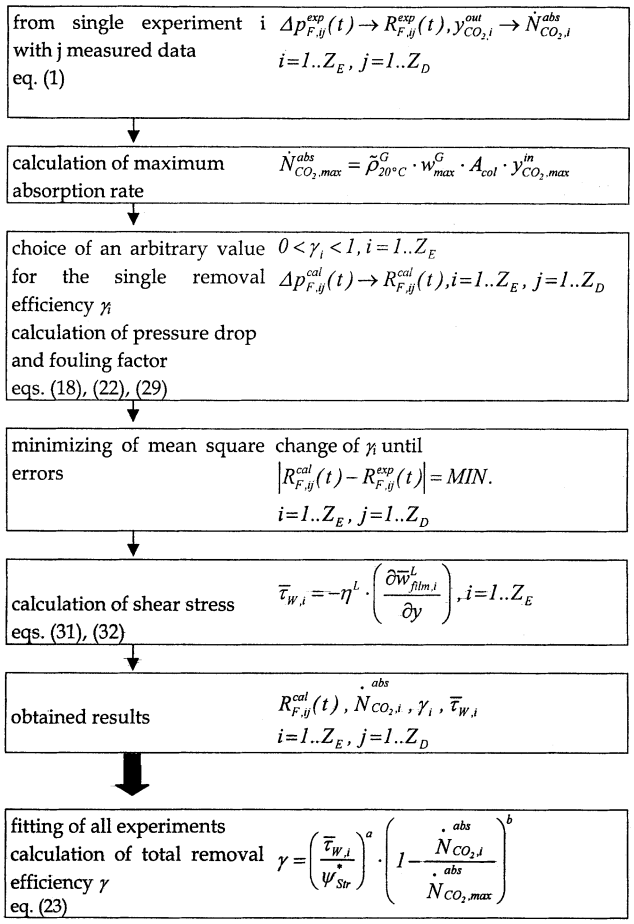

Figure 3. Procedure for obtaining the total removal efficiency factor γ from experimental data.

ing, case (I) from Table 1 is dropped. As shown in Figure 3, the necessary total removal efficiency factor, γ, is obtained from fitting the experimental data.

The experimental fouling factor, $R_{F,ij}^{\exp}(t)$, and the absorption rate, $\dot{N}_{CO_2,i}^{abs}$, can be calculated from all measured pressure drops, j, of one experiment i, $\Delta p_{F,ij}^{\exp}(t)$, at constant operations conditions (constant gas velocity w^G, liquid load u^L and CO_2 concentration $y_{CO_2,i}^{out}$). The total amount of all measured data of one experiment at constant operation conditions is Z_D. The total number of all experiments is Z_E. The maximum absorption rate, $\dot{N}_{CO_2,max}^{abs}$, is obtained by taking the highest measured absorption efficiency and the highest gas velocity at which the mentioned absorption efficiency was measured. Then an arbitrary value of the single removal efficiency γ_i (it refers to one single experiment at constant operation conditions) between 0 and 1 has to be taken and put into the appropriate equations (Eqs. 18, 22 and 29). This yields the value of the calculated fouling factor, $R_{F,ij}^{cal}(t)$. One must change γ_i until the difference between the experimental fouling factor, $R_{F,ij}^{\exp}(t)$, and the calculated fouling factor, $R_{F,ij}^{cal}(t)$, becomes a minimum. The essential mean wall shear stress, $\bar{\tau}_{W,i}$, is to be calculated for every experiment i at constant operation conditions that correspond to the approaches already provided, that is, Eqs. 31 and 32. Finally, all results obtained (as shown in Figure 3) have to be put into Eq. 23, which should combine all experiments at different operation conditions. In this way, a total removal efficiency γ is obtained. This is valid for one packing type.

By using an approximation, it is possible to find several different sets of values, a, b, and ψ_{Str}^*, that might lead to similar results with few differences between experimental and calculated values.

Results and Discussion

Using the developed model, it has been possible to find single removal efficiencies, γ_i, for single experiments (Figures 4–6) as well as the total removal efficiency, γ, for all experiments. In Figure 7, the total removal efficiency, γ, is plotted against the single removal efficiency, γ_i. All appropriate measured data are provided in Tables 3 to 5.

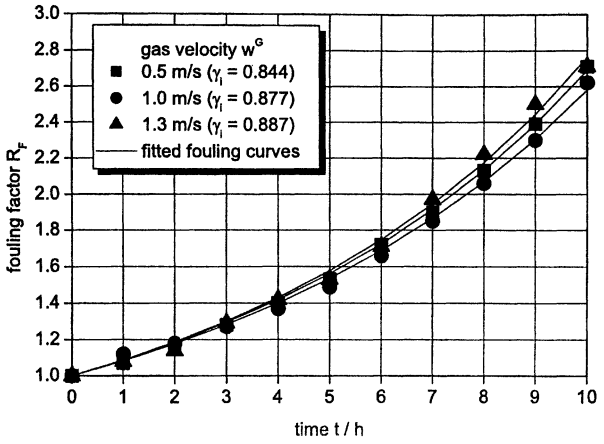

Figure 5. Fouling factor R_F and single removal efficiency γ_i as a function of w^G at constant u^G = 16.98 m³/(m²·h), $y(CO_2)_{in} \approx$ 2,000 ppm.

Figure 4 shows, on the one hand, that the higher the liquid load, the lower the fouling factor when the liquid load, u^L, is increased from 28.29 m³/(m²·h) to 39.61 m³/(m²·h). This is caused by a higher liquid shear stress. On the other hand, the fouling factor increases a little when the liquid load is increased from 16.98 m³/(m²·h) to 28.29 m³/(m²·h). Here deposit formation occurs faster because of the higher absorption rate due to the higher liquid load. Thus, adhesion is assumed to be more dominant than removal. The deposit formed might have a higher adhesiveness and shearing strength.

Figure 5 shows the influence of the gas velocity on the fouling factor at a low liquid load of 16.98 m³/(m²·h). The differences among the measured data are small. The absorption rate (which can be calculated from the gas velocity, CO_2-inlet concentration, and the absorption efficiency) shows

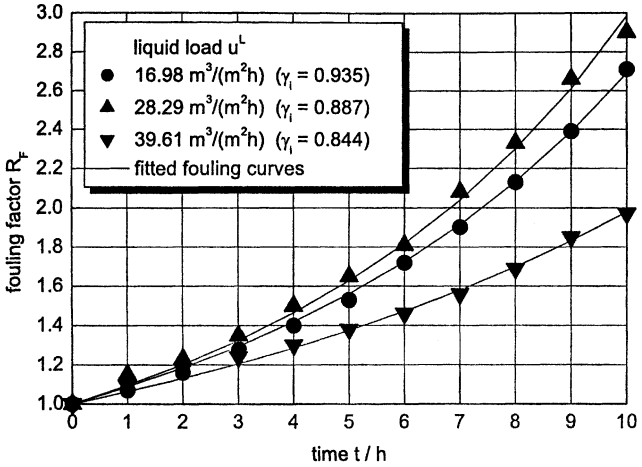

Figure 4. Fouling factor R_F and single removal efficiency γ_i as a function of u^L at constant w^G = 0.5 m/s, $y(CO_2)_{in} \approx$ 2,000 ppm.

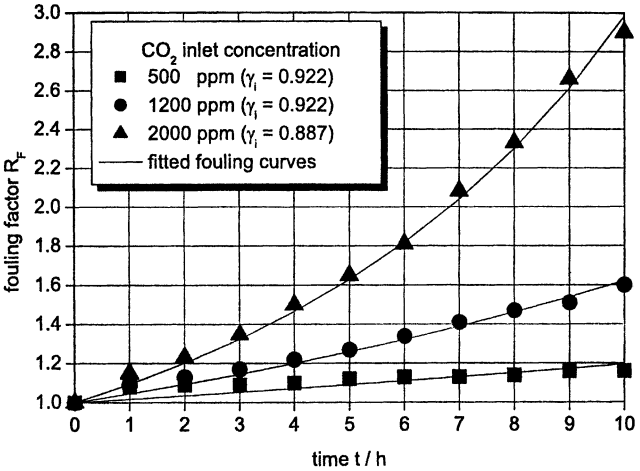

Figure 6. Fouling factor R_F and single removal efficiency γ_i as a function of $y(CO_2)_{in}$ at u^G = 28.29 m³/(m²·h) and w^G = 0.5 m/s.

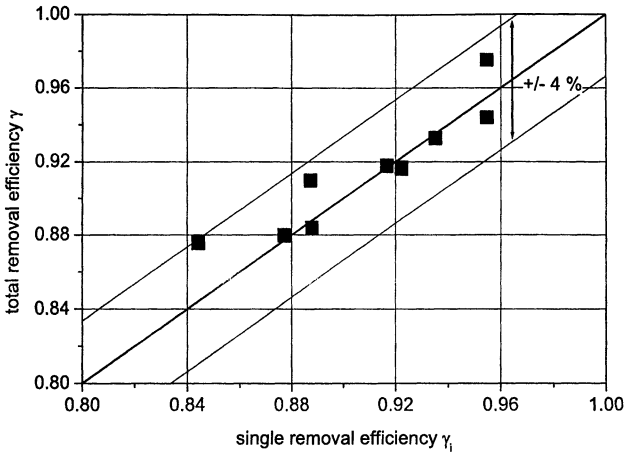

Figure 7. Deviations of the total removal efficiency γ from the single removal efficiency γ_i referred to the packing-type Rauschert Hiflow 15-7 PP.

Table 3. Measured Pressure Drops at Different CO_2-Inlet Concentrations, Constant $w^G = 0.5$ m/s and $u^L = 28.29$ m^3/(m^2·h)

	Pressure Drop $\Delta p(t)$/Pa		
Time (h)	500 ppm	1,200 ppm	2,000 ppm
0	0.67	0.90	0.85
1	0.73	0.98	1.00
2	0.73	1.02	1.07
3	0.73	1.05	1.16
4	0.74	1.10	1.28
5	0.75	1.14	1.41
6	0.76	1.21	1.55
7	0.76	1.27	1.81
8	0.77	1.32	2.00
9	0.78	1.36	2.16
10	0.78	1.44	2.40

almost no dependence on the gas velocity. Nevertheless, different values of γ_i can be found in the range of 0.844 to 0.887.

The influence of the carbon dioxide inlet concentration on the fouling factor can be seen in Figure 6. It is clear that the more CO_2 there is in the inlet stream, the more limestone is formed per time, due to the chemical reaction just mentioned. At lower CO_2 concentrations, the γ_i value for the single experiment is constant, namely, 0.922. The single removal efficiency γ_i decreases at higher CO_2 concentrations.

Looking at the definition of the removal efficiency, it is expected that lower values of γ will be obtained with an increasing fouling factor, R_F. But sometimes a different tendency is obtained at certain operation conditions. In Figure 4, the single removal efficiency, γ_i, decreases with increasing fouling factor, R_F, at liquid loads, u^L, from 16.98 m^3/(m^2·h) to 28.29 m^3/(m^2·h). However, at liquid loads u^L, from 28.29 m^3/(m^2·h) to 39.61 m^3/(m^2·h), the single removal efficiency γ_i decreases with a decreasing fouling factor, R_F.

Although γ_i has a physical meaning, the empirical character of γ_i (and of γ) must be reiterated. The mean shear stress and the structure parameter represent hypothetical parameters. At high liquid loads the shear stress forces that contribute to the removal of the deposits dominate in opposition to the absorption rate, which adds to the deposit formation.

The fitting of γ_i yields an excellent result. All measured data could be described very well. In Figure 7, the total removal efficiency, γ, for all of the experiments is plotted as a function of the single removal efficiency, γ_i. The plot is based on data provided in Table 6. The value sets for a, b, and ψ^*_{Str} have been determined by approximation, namely $a = 0.4123$, $b = 0.004258$, and $\psi^*_{Str} = 6.001$ Pa. The average mean deviation from the measured data is lower than 2% (as shown in Figure 7), and the maximum deviation is lower than 4%.

Table 4. Measured Pressure Drops at Different CO_2-Inlet Concentrations and at Constant $w_G = 0.5$ m/s and $y(CO_2)_{in} \approx 2{,}000$ ppm

	Pressure Drop $\Delta p(t)$/Pa		
Time (h)	16.98 m^3/(m^2·h)	28.29 m^3/(m^2·h)	39.61 m^3/(m^2·h)
0	0.71	0.88	1.05
1	0.76	1.01	1.14
2	0.82	1.08	1.24
3	0.90	1.18	1.30
4	0.99	1.31	1.36
5	1.08	1.45	1.44
6	1.22	1.58	1.52
7	1.34	1.83	1.64
8	1.51	2.04	1.77
9	1.69	2.33	1.93
10	1.91	2.54	2.15

Table 5. Measured Pressure Drops at Different Gas Velocities, Constant $u^L = 16.98$ m^3/(m^2·h) and $y(CO_2)_{in} \approx 2{,}000$ ppm

	Pressure drop $\Delta p(t)$/Pa		
Time (h)	0.5 m/s	1.0 m/s	1.3 m/s
0	0.71	2.39	5.37
1	0.76	2.67	5.79
2	0.82	2.83	6.12
3	0.90	3.04	6.91
4	0.99	3.28	7.62
5	1.08	3.57	8.22
6	1.22	3.98	9.18
7	1.34	4.43	10.59
8	1.51	4.91	11.89
9	1.69	5.50	13.40
10	1.91	6.27	14.54

Table 6. Fitted Single and Total Removal Efficiencies and Measured vs. Calculated Fouling Factor at $t = 10$ h for the Packing-Type Rauschert Hiflow 15-7 PP

w^G m/s	u^L m^3/(m^2·h)	γ_i	γ	$\left(\frac{R_{F,cal}(\gamma)}{R_{F,exp}}\right)\cdot 100$ (%)
0.5	16.98	0.844	0.876	0.79
1.0	16.98	0.877	0.880	1.58
1.3	16.98	0.887	0.884	1.85
0.5	28.29	0.887	0.916	2.80
1.0	28.29	0.910	0.918	1.17
0.5	39.61	0.935	0.933	0.45
1.0	39.61	0.945	0.944	2.17

Conclusion

A new model has been developed to describe fouling in packed columns. The model includes three steps: (1) an approach for pressure drops in packed columns due to the Darcy–Weisbach law; (2) a kinetic approach for the growing of fouling deposits; and (3) introduction of a removal efficiency. The removal efficiency represents a new and a very important approach. The model has been improved by correlating the total removal efficiency, γ, with the single removal efficiencies, γ_i, and mean shear stresses.

Both in experiments and in the presented model, only a part of the total amount of product generated, $\dot{m}_F/\dot{m}_P$, forms a deposit on the packing. Removal effects were not considered in the previous investigations of Chen et al. (1995).

The introduced shear stress and structure parameter needed for describing the single removal efficiency and the total removal efficiency are basically physical properties. Because of the great difficulty in describing and measuring the interactions of the removal and adhesive forces between the packing surface and the solid and between the solid particles, those physical properties are seen as hypothetical parameters.

The correlation equation suggested for the removal efficiency includes only three adjustable parameters. The structure parameter was kept constant because we don't know enough about it.

The fitting has worked very well. The average mean deviation from the measured data is less than 4%. A simple algorithm was used for the fitting. So for the first time, a new and easy approach for describing complex fouling phenomena in packed columns has been provided.

The model is assumed to be transferable to other packings and substances. In the future, it is essential to extend the proposed modeling by more in-depth investigation of adhesion mechanisms, adhesiveness and shearing strength of deposits, and precipitation interacting with nucleation and crystal growth on surfaces.

Acknowledgment

Ms. Stephanie Cardin, Atlanta, GA (USA) is gratefully acknowledged for her careful review of the manuscript.

Notation

a, b = adjustable parameters
a_{eff} = effective specific packing surface, m^2/m^3
A_{geo}, a_{geo} = dry geometrical packing surface, specific packing surface, m^2/m^3
A_{cql} = cross-section area, m^2
B^L = nondimensional liquid load
d_P = particle diameter, m
d_h = hydraulic diameter, m
F^G = F-factor, gas loading factor, $Pa^{0.5}$
H = packing height, m
K = wall factor
N_{Ch} = number of channels
$\dot{N}_j^{\text{abs}}$ = absorption rate, mol/s
m = correlation parameter for nondimensional liquid load B^L
$\dot{m}_F$, $\dot{m}_d$, $\dot{m}_r$ = net mass fouling rate, deposition rate, removal rate, kg/s
M_P = molar mass of component P, kg/mol
Δp = pressure drop, Pa
r_h, $r_{h,\text{eff}}$ = hydraulic radius, effective hydraulic diameter, m
R_F, $\dot{R}_F$ = fouling factor, fouling rate
$R_{F,\text{exp}}$, $R_{F,\text{cal}}$ = fouling factor from experiment, fouling factor from calculation
S_j = mass specific saturation concentration, kg component j/kg solvent
t = time, s
u^L = liquid load, $m^3/(m^2 \cdot h)$
V = volume, m^3
V_{tot} = total volume, m^3
V^L = total volume of liquid holdup, m^3
w^G = gas velocity, m/s
x_F = thickness of deposit, mm

Greek letters

γ_i, γ = single removal efficiency, total removal efficiency
δ = liquid film thickness, m
ϵ, ϵ_{eff} = porosity, effective porosity
ϵ_{abs} = absorption efficiency
η = dynamic viscosity, Pa·s
λ = general drag coefficient
ρ, $\tilde{\rho}$ = density, mole density, kg/m^3, mol/m^3
τ_W, $\bar{\tau}_W$ = shear stress, mean shear stress, Pa
ν^L = liquid kinematic viscosity, m^2/s
ψ = general drag coefficient referred to a packing
$(\psi^{GL})^*$, ψ^{GL} = drag coefficient for two-phase flow, "pseudo" drag coefficient for two-phase flow referred to a packing
ψ^*_{Str} = adjustable structure parameter, Pa
$\dot{\Pi}_r$, $\dot{\Pi}_d$ = general removal and deposition term used for heat exchangers

Superscripts and subscripts

abs = absorption
bottom = concerns the storage and feed tank of the column at the bottom
cal = calculated
CF = crystallization fouling
Ch = channel
eff = effective
exp = experimental
F = fouling
geo = geometrical
G, L = gas, liquid phase
PF = precipitation fouling
max = maximum
0 = start point

Literature Cited

Billet, R., and M. Schultes, "Updated Summary of the Calculation Method of Billet and Schultes," *Trans. Inst. Chem. Eng.*, **77**, 498 (1999).

Bornhütter, K., and A. Mersmann, "Mass Transfer in Packed Columns: The Cylinder Model," *Chem. Eng. Technol.*, **16**, 46 (1993).

Bott, L. F., *Fouling of Heat Exchangers*, Elsevier, Dordrecht, The Netherlands (1995).

Brauer, H., and D. Mewes, "Strömungswiderstand sowie Stoff- und Wärmeübergang in ruhenden Füllkörperschüttungen," *Chem. Ing. Tech.*, **44**, 93 (1972).

Bravo, J. L., "Effectively Fight Fouling of Packing," *Chem. Eng. Prog.*, **89**, 72 (1993).

Chen, G. X., A. Afacan, and K. T. Chuang, "Fouling of Sieve Trays," *Chem. Eng. Commun.*, **131**, 97 (1995).

Crittenden, B. D., and S. T. Kolaczkowski, "Mass Transfer and Chemical Kinetics in Hydrocarbon Fouling," *Proc. Conf. Fouling—Science or Art?*, Institute of Correction Science and Techneaques and the Institute of Chemistry and Engineering, London, p. 169 (1979).

Crittenden, B. D., S. T. Kolaczkowski, and I. L. Downey, "Fouling of Crude Oil Preheat Exchangers," *Trans. Inst. Chem. Eng.*, **70**, 547 (1992).

Epstein, N., "Thinking About Heat Transfer Fouling: A 5 × 5 Matrix," *Heat Transfer Eng.*, **4**, 43 (1983).

Heberle, A., and K. Schaber, "Fouling in einer Absorptionskolonne," *Chem. Ing. Tech.*, **73**, 347 (2001).
Hirsch, H. R., "Scher- und Haftfestigkeit kristalliner Foulingschichten auf wärmeübertragenden Flächen," PhD Thesis, Technical Univ., Braunschweig, Germany (1997).
Mackowiak, J., *Fluiddynamik von Kolonnen mit modernen Füllkörpern und Packungen für Gas/Flüssigkeitssysteme*, Otto Salle, Frankfurt (1991a).
Mackowiak, J., "Pressure Drop in Irrigated Packed Columns," *Chem. Eng. Process*, **29**, 93 (1991b).
Martin, J. F., "Reduce Olefin Plant Fouling," *Hydrocarbon Proc.*, **11**, 63 (1988).
Schaber, K., "Gaswaschanlagen für saure und basische Abgase unter Berücksichtigung der neuen TA-Luft," *Chem. Ing. Tech.*, **59**, 376 (1987).
Söhnel, O., and J. Garside, *Precipitation— Basic Principles and Industrial Applications*, Butterworth-Heinemann, Oxford (1992).
Taborek, J., T. Aoki, R. B. Ritter, J. W. Palen, and J. G. Knudsen, "Fouling: The Major Unresolved Problem in Heat Transfer," *Chem. Eng. Prog.*, **68**, 59 (1972a).
Taborek, J., T. Aoki, R. B. Ritter, J. W. Palen, and J. G. Knudsen, "Predictive Methods for Fouling Behavior," *Chem. Eng. Prog.*, **68**, 69 (1972b).
Manuscript received Nov. 21, 2001, and revision received May 29, 2002.